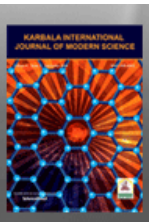

Karbala International Journal of Modern Science

Volume 6 | Issue 2 Article 14

Evaluation of structure and properties of various sol–gel nanocoatings on biomedical titanium surface

Mohsin Talib Mohammed
Mechanical Engineering Department, Faculty of Engineering, University of Kufa, Najaf, Iraq,
mohsint.alyasiri@uokufa.edu.iq

Sarah Mohammed Hussein
Materials Engineering Department, Faculty of Engineering, University of Kufa, Najaf, Iraq, saram.alrwaf@uokufa.edu.iq

Evaluation of structure and properties of various sol–gel nanocoatings on biomedical titanium surface

Abstract

This study deals with the preparation and characterization of different bioceramic nanofilms formed on the surface of new metastable β-titanium (Ti) alloy. The films of pure TiO_2, pure HA, TiO_2/HA bilayer and HA/TiO_2 composite were coated successfully on Ti surface by sol-gel using spray pyrolysis deposition technique. The surface characteristics of coated substrates, such as thickness, topography, morphology, phase transformations and wear behavior, were evaluated and compared to uncoated substrate. The results showed that the sol-gel is a promising technique to create biocoatings on Ti surface with outstanding structure and properties for biomedical applications.

Keywords

Biomedical applications, nanocoating, sol-gel, titanium, wear

Cover Page Footnote

Acknowledgements: The authors of this work would like to sincerely acknowledge the Government of Iraq, Ministry of High Education and Scientific Research, University of Kufa. Also, many thanks to DMRL, Hyderabad, India for manufacturing titanium alloy.

1. Introduction

The use of metallic implants in the medical field has become prevalent in recent times, where they should withstand significant mechanical stresses [1]. In particular, Ti and its alloys are extensively applied for orthopaedic and dental applications due to their outstanding characteristics such as specific strength, better fracture toughness, low elastic modulus as well as excellent corrosion resistance and biocompatibility. It has been proved that Ti and its alloys have higher acceptability by human body tissue than other metallic materials [2]. A great attention from scientists and researchers has been paid to many biocompatible β-type Ti alloys as this kind of Ti alloys can mitigate the effect of stress shielding and lead to exceptional biocompatibility. However, the structure and properties of these alloys still need to be improved to meet the severe conditions of the human body for various medical uses [3].

It is well known that Ti has an ability to form a passive oxide film on its surface with thickness reaches to 1−10 nm [4]. The outstanding surface properties of Ti alloy under human body environment can be achieved due to the simultaneous formation of this thin surface film. However, wear characteristics of Ti are still unsatisfactory [5]. Consequently, wear and friction of Ti implants are imperative issues as they have direct surface contact with bone tissue. Therefore, numerous biological problems, such as bone loss, inflammation and cytoxicity, could be induced due to the formation of wear debris in contact area [6]. Functional ceramic coating over the surface of Ti implant is a substantial technique to enhance its required properties, especially biocompatibility, corrosion and wear [7]. In recent years, much interest was paid to apply sol−gel as a vital coating method, due to its simplicity and capability to coat intricate shapes. Different biocompatible ceramic films have been developed by sol−gel such as titania (TiO_2), hydroxyapatite (HA) and others. Regardless of its higher biocompatibility, HA has a low fracture toughness and a brittle nature, which could lead to early failure to deposited film [7]. Also, the difference in thermal expansion coefficients between Ti substrate and HA coating may cause a decrease in bonding strength between them. Therefore, TiO_2 film was coated onto Ti surface to increase the bonding strength between HA and Ti [8]. The use of high-quality coatings embedded with various compatible nanoparticles in higher purity and exceptional crystallinity is also required to improve the mechanical properties of biomaterials [9]. Moreover, it was reported that the bioactivity, osseointegration, antibacterial properties along with corrosion and tribological resistances can be improved significantly using TiO_2 as a successful alternative protective coating over Ti surface [10].

In the present study, sol−gel coating technique using spray pyrolysis deposition was utilized to coat new metastable β-type Ti alloy with pure TiO_2, pure HA, bilayer TiO_2/HA and composite HA/TiO_2. The structural characterizations of the resulting coatings along with their effect on the micro-hardness and wear behaviour of the investigated Ti alloy were also evaluated and compared to uncoated substrate.

2. Materials and methods

In this study, a new as-cast metastable β Ti−15Zr−12Nb (TZN) alloy was employed as a substrate for different sol−gel processes. This alloy was produced using a non-consumable vacuum arc melting technique existing at DMRL, India. Primarily, the casting process started with a good mixing of raw materials (sponge Ti, Zr chips and Nb powder) under ultrahigh purity argon gas. The melting process was repeated many times to obtain compact and homogeneous Ti ingots. More details about the production of this TZN alloy were mentioned in some works [11,12]. Samples of size 10 × 10 × 3 mm from TZN alloy were used as main substrates in this investigation. The first step is grinding of samples by silicon carbide papers (120−1200) grit, ultrasonically cleaned by ultrasonic cleaner for 15 min using a mixture of ethanol and distilled water and then dried in air. All details related to preparing coating solutions and sol−gel films by spray pyrolysis deposition method for TiO_2, HA, bilayer and composite coatings were mentioned elsewhere [13,14].

Scanning electron microscopy (SEM-FEI Quanta model, Holland) was used to identify the surface structure and the morphology of the coated substrates. The elemental composition of coated surfaces was analyzed using energy dispersive spectroscopy (EDS), which is connected with SEM device as an accessory. Also, the phase transformations of the coated substrates were determined by X-ray diffraction test (XRD-6000, Japan). The parameters of this test were:

https://doi.org/10.33640/2405-609X.1630

CuKα radiation (λ = 0.154056 nm), current 30 mA, voltage 40 KV, 2θ between (10°–80°) and scan speed 8.0000 (deg/min). The surface morphology including 2D and 3D images of uncoated and coated substrates was observed by atomic force microscopy AFM (NTMDT, NTEGRA prima, Russia). The average thickness of different five points for each coating layer was measured using a digital coating thickness gauge type (List-Magnetik Mega-Check Pocket) in an accuracy of ±0.1 μm. Vickers micro-hardness was measured using an automatic micro-hardness tester (TH715, Beijing Time High Technology Ltd). The micro-hardness test was repeated five times for each substrate using a load of 9.8 N and a dwelling time of 15s. The wear performance of uncoated and coated TZN alloy substrates was analyzed using a reciprocating pin-on-disc sliding wear tester (MICRTEST, S. A., Spain) under dry condition at room temperature. The applied normal force, sliding distance, sliding velocity and speed of wear test were selected to be 1 N, 75 m, 200 rpm and 10 mm s^{-1}, respectively. The wear resistance of uncoated and coated TZN alloy substrates was analyzed depending upon the measured coefficient of friction (COF), weight loss and wear rate. Besides, SEM observations were used to evaluate the worn surfaces of uncoated and coated TZN alloy substrates.

3. Results and discussion

3.1. Thickness and AFM measurements

The thickness of the coating is an important factor which has a significant effect on the performance of coated Ti substrates. The thickness values of TiO_2, HA, bilayer and composite coatings were measured to be 34, 22, 59 and 41 μm, respectively.

Fig. 1(a–e) shows the AFM images of uncoated and coated TZN alloy substrates. Fig. 1a revealed that the uncoated substrate has lower value of Ra (9.495 nm) compared to that of coated substrates. This indicates the significant effect of different coatings produced by sol–gel process on TZN alloy surface. On the other hand, the AFM analysis showed that the coated substrates are fully covered by nano-scale layers. In case of TiO_2, the film is composed of nano-particles with an average grain size of about 101 nm. The topography of this coating characterizes porous structure and rough surface, with higher value of Ra (30.417 nm). This might be owing to the existence of high amount of micropores and bigger agglomerations along with a decrease in homogeneity, as shown in Fig. 1b. It is important to mention here that the rough and porous

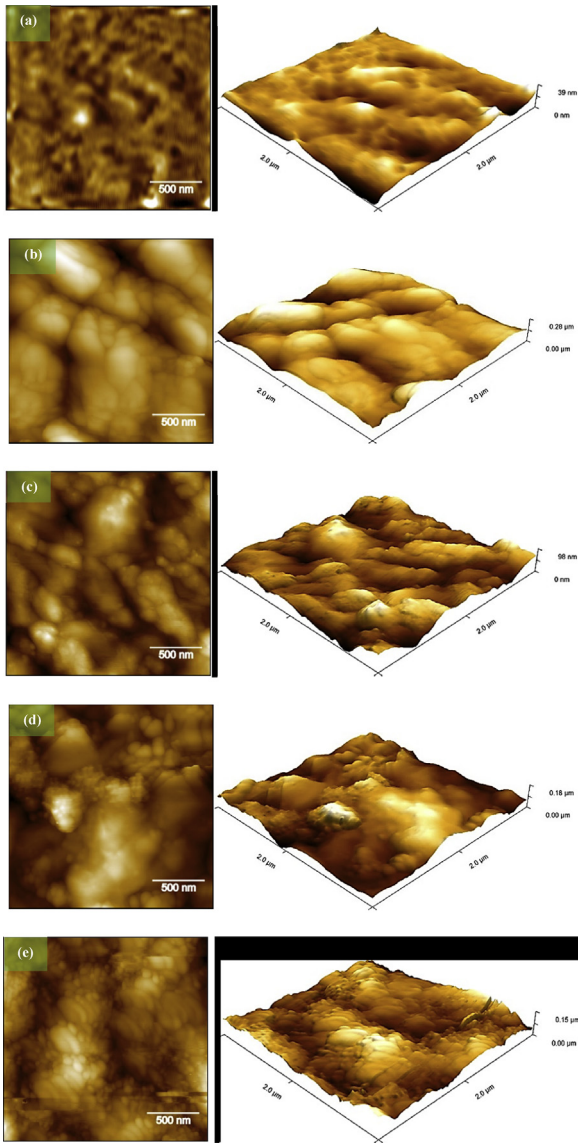

Fig. 1. AFM topography images under different presentation mode and resolutions of: (a) uncoated, (b) TiO_2, (c) HA, (d) bilayer and (e) composite coated substrates.

structure of TiO_2 film might increase the coating adhesion of the subsequent HA layer in bilayer coating. In case of HA coating, the film is composed of nano-particles with an average grain size of about 96.8 nm, as shown in Fig. 1c. The topography of this coating characterizes porous structure with a higher value of Ra (16.529 nm) compared to uncoated substrate, but it is lower than that of TiO_2 coated substrate. The presence of higher amount of porosity and agglomeration along with reduced homogeneity in structure is the main factor affected on the surface

roughness of HA coating. The topography of bilayer discloses nanoscale structure with a greater homogeneity and smaller particle size (62.5 nm), as shown in Fig. 1d. The surface of this coating is smother (Ra = 17.213) than TiO_2 film and comparable to HA film as it possesses less amount of porosity. It can be seen from Fig. 1e that TiO_2 is highly integrated with HA particles in composite coated substrate. Also, a nanoscale structure with a higher homogeneity and smaller particle size (65.1 nm) is obtained in composite coating. However, the composite film has a comparable surface roughness (Ra = 19.559) to that of bilayer and HA coatings, along with lesser levels of porosity in comparison to other coatings. It was pointed out that the rapid attachment of the oesteoblast cells onto the implant surface can be achieved by increasing the surface roughness, which may provide a substantial improving in contact area with the bone [15]. Consequently, it is expected that the coated substrates in this study induce essential developments in the bioactivity and bone bonding ability.

3.2. SEM-EDS observations

Fig. 2 exhibits SEM micrographs and EDS analysis of TiO_2, HA, bilayer and composite coatings. According to the present SEM observation, no noticeable fracture is observed in the surfaces coated by TiO_2 and bilayer films. In Fig. 2 (a), the surface is totally covered with pure TiO_2 coating, consisting mainly of nanosized particles and different irregular clusters together with some detectable micro-cracks distributed on this film. The coalescence of the nanoparticles was developed to form coarse particles and large grains in an irregular distribution. The formation of a cracked surface is owing to mutual effect of contraction and stress resulted from the different thermal expansion between TiO_2 and TZN alloy during the thermal treatment of sol–gel process, or as a result of the evaporation of solvent molecules during sintering process [16]. Moreover, a high density of obvious grain boundary micro-pores was observed within the microstructure of pure TiO_2 coating. These pores were bigger and more abundant in the surface, resulting in a well consolidated macro-porous layer with higher biofunctionality. The movement of human body fluid throughout the pores might enhance the cell infiltration process, which in turn supports the formation of new bone cells. Also, the more attachment points for osteoblast adhesion and differentiation may be resulted from these pores formed in bioceramic coatings [17]. The corresponding EDS analysis of TiO_2 film shows the major elemental peaks of Ti and O, which confirms the formation of TiO_2 coating. It can be observed from Fig. 2 (b) that the surface is entirely covered with uniform deposition of pure HA film. The surface of HA coated substrate has irregular crystallite aggregates in plate-like shape with a thickness of 1–4 μm in various orientations. These structural aggregates can be explained as a coalescence of many nanoparticles developed on the coated surface. Also, some detectable micro-cracks distributed on HA film were observed, which was resulted from the significant difference in thermal expansion between coating and substrate [16]. Moreover, sponge-like structure or porous structure was observed within the microstructure of pure HA film, which consists of numerous nano- and micro-pores (0.2–2 μm) in an obvious grain boundary. It is important to mention here that a heterogeneous nucleation of the apatite particles can be promoted with the formation of the cracks and/or porosity in the morphology of HA coating layer. These apatite particles have a higher tendency to fill the cracks throughout their continuous growth [18]. The corresponding EDX spectrum for HA coating shows that the apatite layers were successfully synthesized on the surface of TZN alloy. It confirmed the formation of HA coating with the existence of distinct peaks of Ca, P, O and Ti, which are related to the main elements of HA coating and TZN alloy substrate. Furthermore, the Ca/P atomic ratio of deposited HA film is 1.62 which is very closer to the theoretical value of HA in human bone structure (1.67). In Fig. 2 (c), the microstructure of bilayer surface is homogeneous, compact and dense intact coating nature. It essentially consists of more apparent nano granular-like particles. Also, a considerable decrease in the amount of porosity and in the dimensions of pores was noted on the surface comparing with that of pure TiO_2 and HA films. It is important to mention here that the biocompatible nanometer TiO_2, as an intermediate layer, could promote the controlled interaction and the bonding strength of the bioactive HA film into the surface of the TZN substrate. In addition, this bioceramic layer may assist in increasing the bioactivity and inhibiting the erosion of the outer HA layer after its resorption or degradation [19]. The cracked surface obtained in first layer of pure TiO_2 (Fig. 2a) is more favorable for developing the quality of the deposition of HA coating and increasing the adhesive strength between the first layer (TiO_2) and the final layer (HA). The micro-cracks formed on TiO_2 layer through the shrinkage happened during calcination treatment can act as vital points of "mechanical interlocking" which may eventually lead

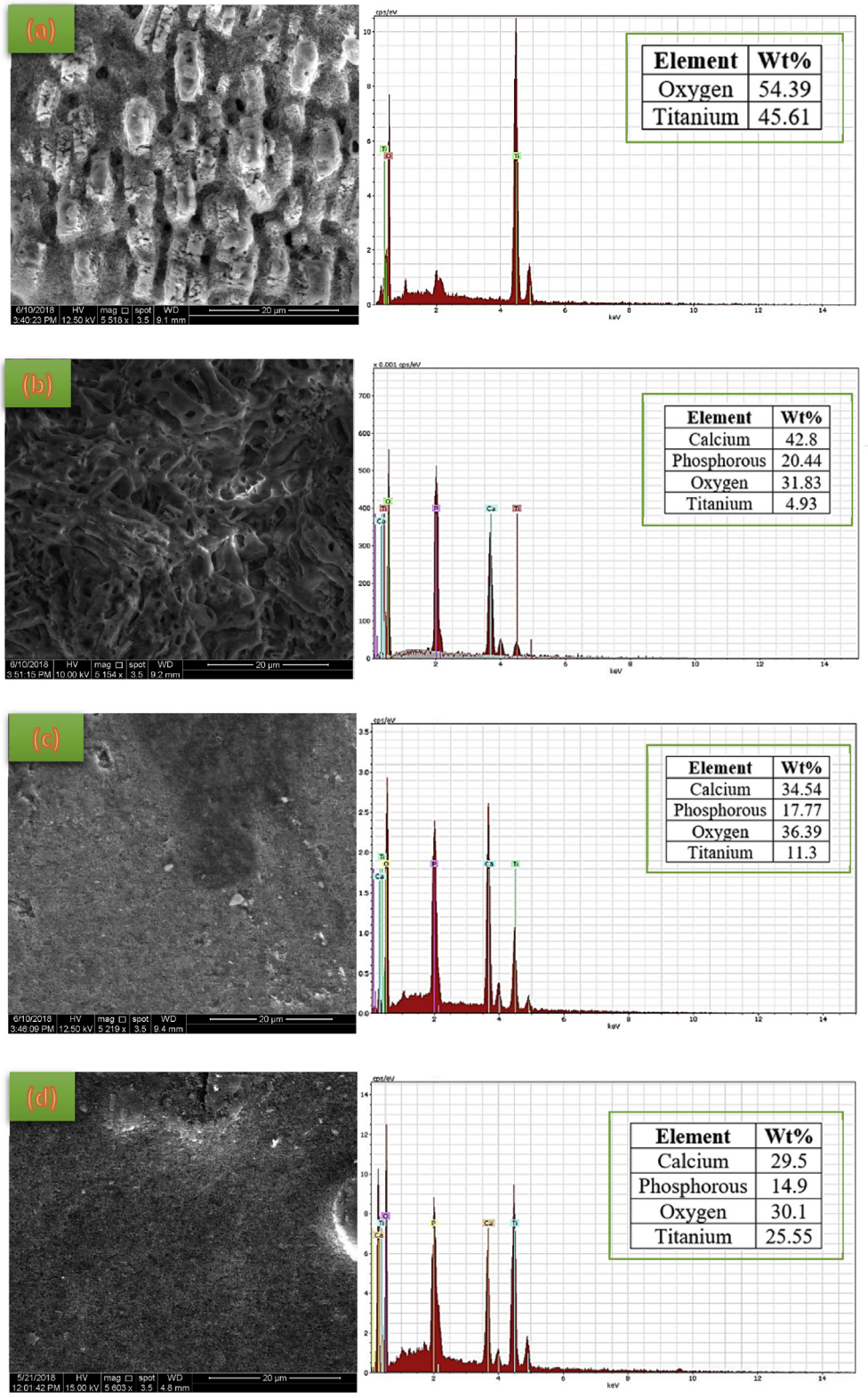

Fig. 2. SEM images (left) and point EDS spectrum (right) of (a) TiO_2, (b) HA, (c) bilayer and (d) composite coated substrates.

to improve the osteintegration [20]. Therefore, the final HA film blocked the cracks and covered entirely the surface of the TiO_2 film. The EDX spectrum evidently shows the existence of P, Ca, and O, the main constituents of HA layer. The small weight percentages of phosphorus (17.77 Wt %) and calcium (34.54 Wt %) confirm that the deposited HA is a thin film. The Ca/P ratio was measured to be 1.502. Fig. 2 (d) showed that the composite coated surface has a regular thin porous structure with higher compact and homogeneity. The enhanced homogeneity of coated surface is attributed to good incorporation of TiO_2 with HA matrix. This film consists mainly of nano granular-like particles with regular nano- and micro-pores. Moreover, a significant decrease in the dimensions of pores was observed in the structure of composite film compared to that of TiO_2 and HA. These morphological results are very identical with previous results of AFM analysis (Fig. 1). Moreover, these vital results have a good agreement with the results obtained from literature [19]. The EDS spectra revealed that the composite film has Ca/P ratio of 1.53. The existence of strong peaks related to Ti and O along with Ca and P peaks confirms the formation of HA and TiO_2 in composite coating. Furthermore, peaks other than HA and TiO_2 were not seen, which confirms the purity of the coating. Thus, it can be concluded that TiO_2 phase was well embedded into HA matrix.

3.3. X-ray diffraction analysis

The crystal structures of uncoated substrate along with TiO_2, HA, bilayer and composite coatings were characterized using XRD analysis, as shown in Fig. 3. The XRD profile of uncoated substrate indicates the formation of main two phases in Ti alloys, i.e. α (JCPDS 44−1294) and β (JCPDS 44−1288) phases. For pure TiO_2 layer, sharp and strong intense peaks attributed to anatase TiO_2 (JCPDS 00-029-1360) were detected. It was pointed out that the anatase phase possesses a greater bioactivity than that of rutile phase as anatase has lower zeta hydroxyl groups potential, higher lattice match with hydroxyapatite and higher acidity [21]. Similarly, peaks related to rutile TiO_2 (JCPDS 00-021-1276) were also observed. The presence of the rutile phase within the oxide coating proves that the final oxide layer has a stable coating [22]. For pure HA film, several major peaks attributed to HA (JCPDS pattern No. 09−0432) were detected. Furthermore, it can be noted that no sign of calcium oxide or calcium titanate in the XRD analysis of HA coating. However, some diffraction peaks

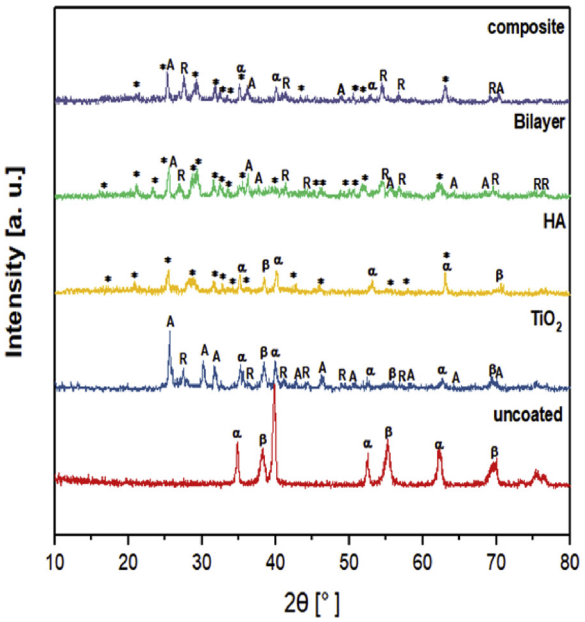

Fig. 3. XRD patterns for uncoated, TiO_2, HA, bilayer and composite coatings.

corresponding to Ti were observed, which probably derived from TZN alloy substrate. For bilayer film, several typical sharp and narrow crystalline HA diffraction peaks were demonstrated. Also, two additional high intensity peaks corresponding to the crystallization of TiO_2 into anatase crystals were noted. Some further high intensity peaks related to the crystallization of TiO_2 into rutile crystals were also indicated. In bilayer coating, it is expected that the microstructural characteristics of final HA layer are significantly dependent on the surface features of the underlying substrate [23]. Consequently, an enhancement in the crystallization of HA was achieved due to the deposition of inner TiO_2 layer. It can be confirmed that great crystallization of titania in anatase and rutile structures within the structure of pure TiO_2 coating was obtained. Whereas, an apatite along with titania in anatase and rutile structures can be noticed in bilayer coating, indicating a substantial development of crystals within this film. For composite film, numerous crystalline HA diffraction peaks were revealed. Also, some main diffraction peaks corresponding to the crystallization of TiO_2 into rutile (JCPDS 00-021-1276) and anatase crystals (JCPDS00-029-1360) were noticed. Here, it is of distinct observation that only the development of titania and apatite phases without the creation of other phases, which confirms the great thermal stability of both titania and apatite structures in

composite coating derived by sol–gel process. The secondary compounds, like calcium oxide, calcium titanium oxides and tricalcium phosphate were not detected in composite film. Moreover, it is expected that the crystallization of HA in composite film can be delayed as a result of mixing HA and TiO_2 in this type of coating, which may cause a formation of weaker HA peaks [24]. Moreover, the decomposition of HA into more soluble phases like tricalcium phosphate (α-TCP or β-TCP) may cause a significant degradation in the mechanical properties of final coating [25]. Therefore, in this work, the temperature of sintering treatment of coating was controlled to be below β-transus temperature of TZN alloy and kept only at 550 °C in order to avoid this undesirable effect. Furthermore, the XRD patterns of composite coating identified some diffraction peaks corresponding to Ti which might be related to TZN alloy substrate.

3.4. Micro-hardness investigation

As is well identified, the biomaterial utilized for long-term implants should possess higher mechanical strength and better biological properties owing to the complex nature of human body environment [26]. Therefore, in this study, the micro-hardness, as one of the mechanical properties required for coated surfaces, was evaluated, and the results of uncoated and coated substrates are represented in Fig. 4. It can be seen from this figure that the hardness of uncoated substrate was 260.6 ± 1.5 HV, which is the lowest value compared with that of coated substrates, but it is higher than that of pure Ti (110 HV). In addition, it can be seen that the composite and bilayer coatings offer the higher hardness values (497.4 ± 4 and 395.4 ± 2 HV, respectively) compared to that of uncoated, TiO_2, and HA. It was reported that the biocompatible ceramic oxide layers deposited by sol–gel process over the surface of implant can substantially improve the surface hardness [9] and reduce the plastic deformation of the coated substrates [6]. Furthermore, the microstructure and the morphology of the surface coating play a key role in determining the values of the surface hardness. The surface coating with adherent crystalline coatings, significant bonding strength and less amount of porosity provides higher hardness values [27]. For bilayer film, the presence of the nanometer intermediate TiO_2 layer played a key role in increasing the interaction and the bonding strength of the final bioactive HA coating onto the surface of TZN alloy substrate and without any detectable micro-cracks or detachment from the substrate (Fig. 2c). For composite film, it was reported that the doping of TiO_2 in HA could enhance the physical reliability between the coating film and the substrate with higher inter-particle bonding [19], which in turn causes a considerable increase in surface hardness. Here, the highest hardness of composite coating is due to the higher bonding strength and the interaction of this film onto the substrate surface as a result of the formation of homogeneous nanometer film without any evident micro-cracks or detachment from the substrate (see Fig. 2d).

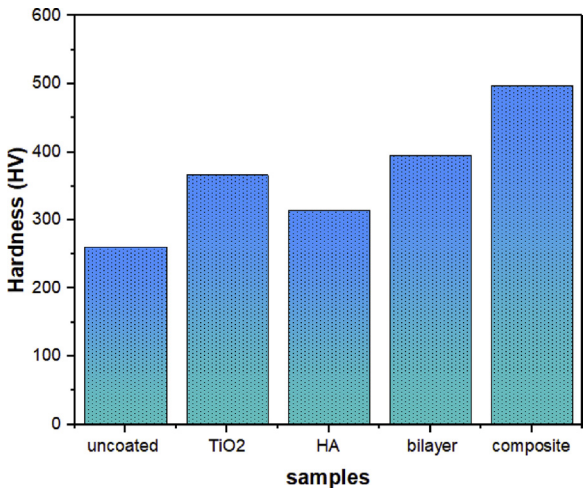

Fig. 4. Surface hardness profiles of uncoated and different coated substrates.

3.5. Wear characteristics

Visual inspection of uncoated and coated TZN alloy substrates showed that during wear tests, the amount of the fractured particles on uncoated surface were higher than that on coated substrates, which may cause an increase in COF. Fig. 5(a, b) demonstrates the COF values and wear rates of uncoated, TiO_2, HA, bilayer and composite coatings. The average values of COF of uncoated, HA, TiO_2, bilayer and composite coatings were 0.82, 0.77, 0.72, 0.55 and 0.49, respectively. It can be seen from Fig. 5 (a) that for all tested substrates, the COF values increase with increasing test period, i.e. a continuous increasing in COF with increasing the residence time of the wear test. The increase of the COF may be related to the formation of wear debris during the friction process, which can cause abrasive wear, leading finally to failure of surface film [28]. Furthermore, the COF values of coated substrates were significantly lower than that of uncoated substrate. The uncoated substrate has the highest value of COF which

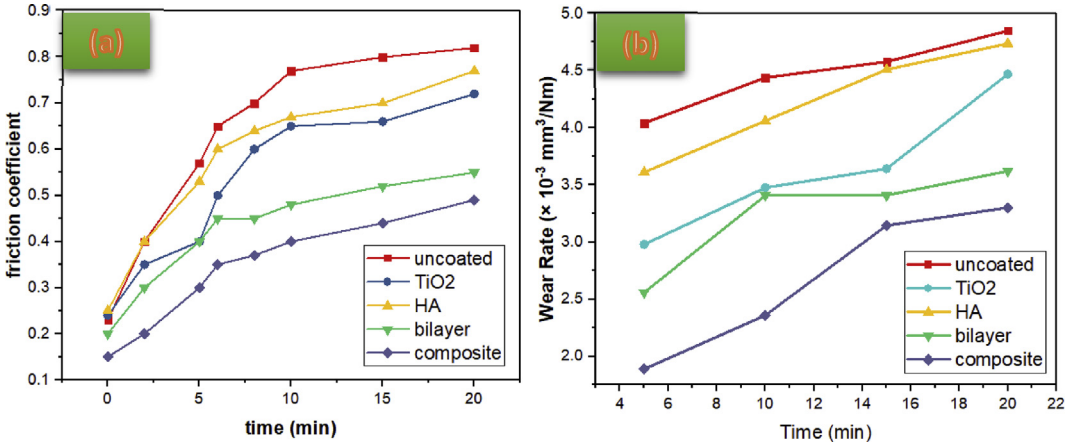

Fig. 5. Friction coefficient values (a) and the wear rate (b) of uncoated, TiO_2, HA, bilayer and composite coatings.

makes it more inferior compared to coated substrates. However, the wear behavior of pure TiO_2 and pure HA coated substrates has an inferior values of COF compared to that of bilayer and composite coated substrates. This reveals the weak effect of pure TiO_2 and pure HA layers in improving the wear resistance of TZN alloy. This unfavourable result may be attributed to the weak interface between these coatings and the surface of TZN substrate as a result of internal micro-cracks formed onto the surface (see Fig. 2a–b). As a result, it may simply induce micro-fracture on the interface and produce abrasive particles, leading to rapid failure of TiO_2 and HA coatings. On the other hand, bilayer coated substrate shows lower COF than pure TiO_2 and pure HA coated substrates after completing the sliding period. This result is due to homogenous nanostructure of the bilayer coating with the higher surface bonding between HA and TiO_2 films (see Fig. 2c). It is worth noting that the composite coated substrate showed the lowest COF value among coated substrates after completing the sliding period. This proves that the composite coated substrate is the highest wear resistance, which surely guides to a longer wear life. This optimal finding is greatly associated with the presence of homogenous and nano-scale structure of composite film with outstanding surface bonding with TZN alloy substrate (see Fig. 2d). Also, it is important to mention here that the significant reduction in COF of composite coated substrate may be resulted from the considerable increase in some vital properties of formed film especially structure stability, surface hardness, film thickness [29] and roughness [30].

Using SEM observations, the worn surfaces of uncoated and coated substrates were evaluated in order to attain more details about the mechanisms of friction and wear. Fig. 6 shows the wear tracks (red arrows) of uncoated, TiO_2, HA, bilayer and composite coatings after completing the wear test. It can be seen that the track width of uncoated substrate (Fig. 6a) is so large to be appeared in a specific magnification used for SEM test, which indicates that this surface suffered from severe adhesive wear and plastic deformation between the pin and substrate during the wear test [31]. In contrast, the coated substrates had narrow track width, which reveals that the wear resistance of TZN alloy is developed after sol–gel process, as shown in (Fig. 6 b-e). In addition, the narrowest wear track was observed on composite coated substrate (Fig. 6e), which indicates that this film has an excellent wear resistance among the coated substrates. This is might be attributed to the high surface hardness and film thickness of composite film compared to other films. Also, the worn surfaces of composite and bilayer coated substrates were relatively smoother than TiO_2 and HA coated substrates. It can be seen that large delamination and plentiful fine wear particles are formed on the surface of TiO_2 and HA (see Fig. 6b and c), indicating the possibility of occurring sudden rupture through wear process. The worn surface images of the bilayer and composite coated substrates showed that an evident deformation occurred on the surfaces, which discloses the best result of the wear resistance. The plastic deformation is may be occurred due to the nano-scale structures of bilayer and composite films (Fig. 2c and d). The deformation is so

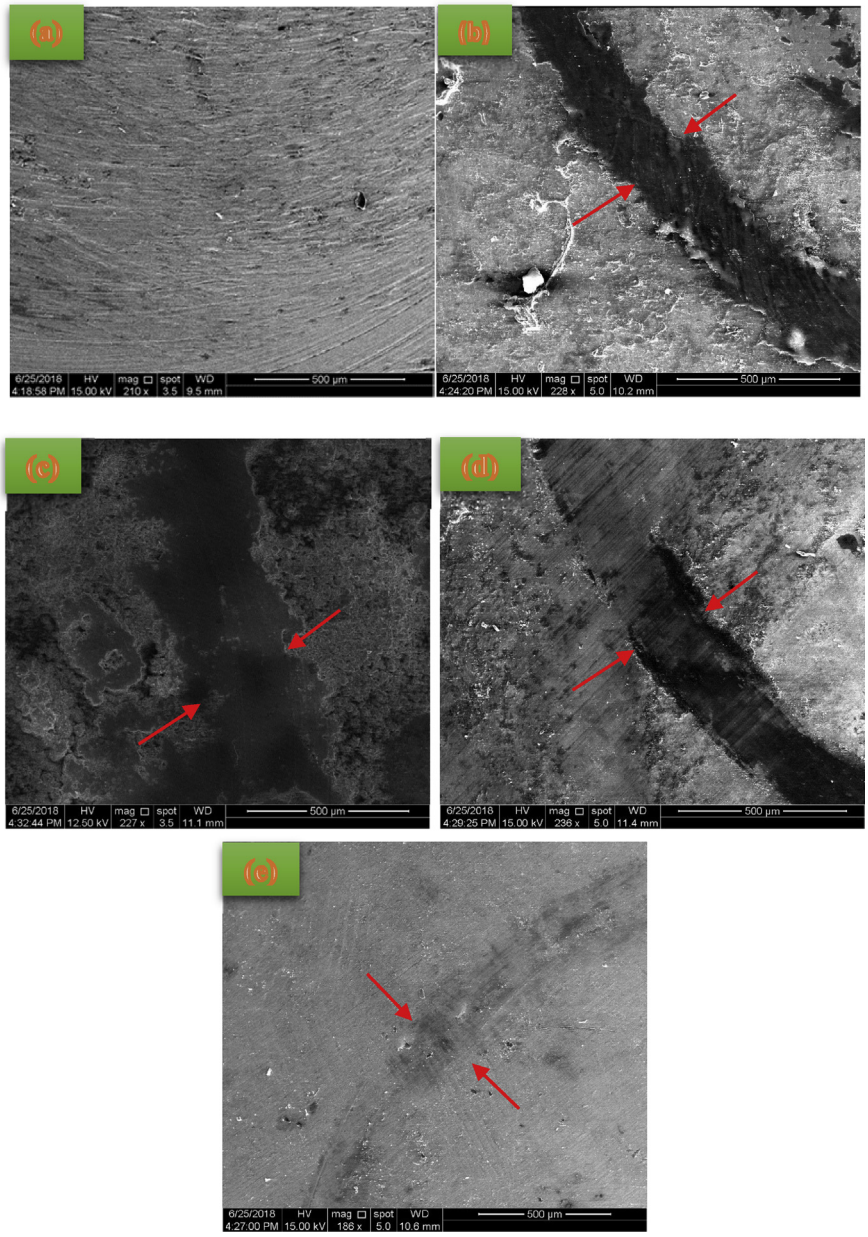

Fig. 6. SEM micrographs of worn surfaces of (a) uncoated, (b) TiO_2 (c) HA, (d) bilayer and (e) composite coatings.

probably responsible for prevention or decrease the potential creation of micro-fractures, which could lead to a significant decrease in COF and abrasive particles. It can be concluded that the wear mechanism of bilayer and composite coated substrates is featured with deformation and abrasive wear without apparent fracture, whereas the wear mechanism of the TiO_2 and HA coated substrate is dominated by microfracture and abrasive wear.

4. Conclusions

In this present work, four different bioceramics coatings, pure TiO_2, pure HA, TiO_2/HA bilayer and HA/TiO_2 composite, were successfully deposited on the surface of a new metastable Ti−15Zr−12Nb alloy using sol−gel technique for biomedical applications. These biocoatings were characterized with respect to microstructure, phase composition, surface

topography, thickness, micro-hardness, and wear properties. The main conclusions of this study can be summarized as follow:

- TiO_2 coating characterizes cracked surface with inferior homogeneity and increased value of roughness. HA film possesses irregular crystallite aggregates in plate-like shape with numerous nano- and micro-pores and some detectable micro-cracks distributed on the surface. While in bilayer, the structure is more homogeneous, smother and denser as cracked surface was completely covered by the consequent HA layer. In contrast, composite film consists mainly of nano granular-like particles and regular nano- and micro-pores in a significant decrease in the dimensions along with compact structure in higher homogeneity without any damage, crack or disintegration.
- XRD analysis reveals that TiO_2 layer has a stable structure in great crystallization. While several major peaks related to the formation of apatite phase were detected in pure HA film. On the other hand, a higher crystalline HA was observed in bilayer without any decomposition of HA into more soluble phases. For composite film, the development of titania and apatite phases without other phases were observed, which confirms the great thermal stability of both titania and apatite structures in composite film.
- The bilayer and composite coated substrates exhibit higher micro-hardness compared to TiO_2 and HA coated substrates.
- The advanced nanostructures of the composite and bilayer films with good hardness values had a significant effect on wear resistance of TZN implant. The wear mechanisms of these coatings were dominated by deformation, abrasive wear and without an obvious fracture.
- Therefore, TZN alloy coated by sol–gel technique can be considered as a very promising biomaterial for hard tissue replacements.

Acknowledgements

The authors of this work would like to sincerely acknowledge the Government of Iraq, Ministry of High Education and Scientific Research, University of Kufa. Also, many thanks to DMRL, Hyderabad, India for manufacturing titanium alloy.

References

[1] M. Catauro, F. Bollino, F. Papale, Biocompatibility improvement of titanium implants by coating with hybrid materials synthesized by sol-gel technique, J. Biomed. Mater. Res. 102A (2014) 4473–4479.
[2] C. Wen, W. Xu, W. Hu, P. Hodgson, Hydroxyapatite/titania sol–gel coatings on titanium–zirconium alloy for biomedical applications, Acta Biomater. 3 (2007) 403–410.
[3] M.T. Mohammed, Z.A. Khan, A.N. Siddiquee, Beta titanium alloys: the lowest elastic modulus for biomedical applications: a review, Int. J. Chem. Nuc. Metall. Mat. Eng. 8 (2014) 726–731.
[4] C. Schvezov, M. Alterach, M. Vera, M. Rosenberger, A. Ares, Characteristics of hemocompatible TiO_2 nano-films produced by the sol-gel and anodic oxidation techniques, JOM 62 (2010) 84–87.
[5] M.T. Mohammed, Z.A. Khan, A.N. Siddiquee, Influence of microstructural features on wear resistance of biomedical titanium materials, Int. J. Chem. Nuc. Metall. Mat. Eng. 7 (2013) 52–56.
[6] I.A. Ovidko, A.G. Sheinerman, Plastic deformation and fracture processes in metallic and ceramic nanomaterials with bimodal structures, Adv. Mat. Sci. 16 (2007) 1–9.
[7] A. Abrishamchian, T. Hooshmand, M. Mohammadi, F. Najafi, Preparation and characterization of multi-walled carbon nanotube/hydroxyapatite nanocomposite film dip coated on Ti–6Al–4V by sol–gel method for biomedical applications: an in vitro study, Mater. Sci. Eng. 33 (2013) 2002–2010.
[8] X. Ji, W. Lou, Q. Wang, J. Ma, H. Xu, Q. Bai, C. Liu, J. Liu, Sol-gel-derived hydroxyapatite-carbon nanotube/titania coatings on titanium substrates, Int. J. Mol. Sci. 13 (2012) 5242–5253.
[9] L.H. Hernández-Gómez, J.F. Pava-Chipol, M. Trejo-Valdez, C. Torres-Torres, J.A. Beltrán-Fernández, G. Urriolagotia-Sosa, C.R. Torres-SanMiguel, Guillermo urriolagotia-calderón, strain measurements exhibited by a steel prosthesis protected with Au nanoparticles, in: A. Öchsner, H. Altenbach (Eds.), Design and Computation of Modern Engineering Materials. Advanced Structured Materials, vol. 54, Springer International Publishing, Switzerland, 2014, pp. 107–120, https://doi.org/10.1007/978-3-319-07383-5_9.
[10] X. He, G. Zhang, X. Wang, R. Hang, X. Huang, L. Qin, B. Tang, X. Zhang, Biocompatibility, corrosion resistance and antibacterial activity of TiO_2/CuO coating on titanium, Ceram. Int. 43 (2017) 16185–16195.
[11] M.T. Mohammed, Development of a new metastable beta titanium alloy for biomedical applications, Karbala Int. J. Mod. Sci. 3 (2017) 224.
[12] M.T. Mohammed, A.A. Diwan, O.I. Ali, Study the formation of porous surface layer for a new biomedical titanium alloy, Mater. Res. Express 5 (2018), 036526, https://doi.org/10.1088/2053-1591/aab4da.
[13] M.T. Mohammed, S.M. Hussein, Synthesis and characterization of nanocoatings derived by sol–gel onto a new surgical titanium surface, Mater. Res. Express 6 (2019), 076426, https://doi.org/10.1088/2053-1591/ab1722.
[14] S.M. Hussein, M.T. Mohammed, Pure and bilayer sol-gel nanolayers derived on a novel Ti surface for load bearing applications, Mater. Today: Proceedings 18 (2019) 2217–2224.

[15] S. Nijhawan, P. Bali, V. Gupta, An overview of the effect of topographic surface modifications of endosteal implants on bone performance and bone implant responses, Int. J. Oral Implant. Clin. Res. 1 (2010) 77−82.

[16] B. Mellor, Surface Coatings for Protection against Wear, first ed., Woodhead Pub., Cambridge, 2016.

[17] C. Ustundag, F. Kaya, M. Kamitakahra, C. Kaya, K. Ioku, Production of tubular porous hydroxyapatite using electrophoretic deposition, The Ceramic Society of Japan 120 (2012) 569−573.

[18] S. Thomas, P. Balakrishnan, M. Sreekala, Fundamental Biomaterials, first ed., Elsevier Science, 2018.

[19] G. He, J. Hu, S. Wei, J. Li, X. Liang, E. Luo, Surface modification of titanium by nano-TiO_2/HA bioceramic coating, Appl. Surf. Sci. 255 (2008) 442−445.

[20] E. Milella, F. Cosentino, A. Licciulli, C. Massaro, Preparation and characterisation of titania/hydroxyapatite composite coatings obtained by sol-gel process, Biomaterials 22 (2001) 425−431.

[21] W. Xia, C. Lindahl, J. Lausmaa, H. Engqvist, Biomimetic hydroxyapatite deposition on titanium oxide surfaces for biomedical application, in: M. Cavrak (Ed.), Advances in Biomimetics, IntechOpen, 2011, pp. 429−452.

[22] T. Yetim, Corrosion behavior of Ag-doped TiO_2 coatings on commercially pure titanium in simulated body fluid solution, Bionic Engineering 13 (2016) 397−405.

[23] D. Sidane, D. Chicot, S. Yala, S. Ziani, H. Khireddine, A. Iost, X. Decoopman, Study of the mechanical behavior and corrosion resistance of hydroxyapatite sol−gel thin coatings on 316L stainless steel pre-coated with titania film, Thin Solid Films 593 (2015) 71−80.

[24] J. Han, Z. Yu, L. Zhou, Hydroxyapatite/titania composite bioactivity coating processed by the sol−gel method, Biomed. Mater. 3 (2008) 455−458.

[25] M. Khodaei, A. Valanezhad, I. Watanabe, R. Yousefi, Surface and mechanical properties of modified porous titanium scaffold, Surf. Coating. Technol. 315 (2017) 61−66.

[26] B. Hahn, J. Lee, D. Park, J. Choi, J. Ryu, W. Yoon, B. Lee, D. Shin, H. Kim, Aerosol deposition of silicon-substituted hydroxyapatite coatings for biomedical applications, Thin Solid Films 518 (2010) 2194−2199.

[27] B. Dikici, M. Niinomi, M. Topuz, Y. Say, B. Aksakal, H. Yilmazer, M. Nakai, Synthesis and characterization of hydroxyapatite/TiO_2 coatings on the β-type titanium alloys with different sintering parameters using sol-gel method, Protect. Met. Phys. Chem. Surface 54 (2018) 457−462.

[28] K. Im, S. Lee, K. Kim, Y. Lee, Improvement of bonding strength to titanium surface by sol−gel derived hybrid coating of hydroxyapatite and titania by sol−gel process, Surf. Coating. Technol. 202 (2007) 1135−1138.

[29] A. Alsaran, Ç. Albayrak, Effect of single and duplex surface treatments on wear properties of CP-Ti, Surf. Eng. 27 (2011) 205−210.

[30] P. Choudhury, D. Agrawal, Sol−gel derived hydroxyapatite coatings on titanium substrates, Surf. Coating. Technol. 206 (2011) 360−365.

[31] B. Sarma, A. Pal, H. Bailung, J. Chutia, Growth of nanocrystalline TiO_2 thin films and crystal anisotropy of anatase phase deposited by direct current reactive magnetron sputtering, Mater. Chem. Phys. 139 (2013) 979−987.